Supporting information

Crystallographic determinations of solid-state structural transformations in a dynamic metal‑organic framework

Gui-Lian Li,[a] Guang-Zhen Liu, [a]Lu-Fang Ma,[a] Ling-Yun Xin,[a] Xiao-Ling Li[a] and Li-Ya Wang*[a,b]*

[a] *College of Chemistry and Chemical Engineering, Luoyang Normal University, Luoyang, Henan, 471022, P. R. China*
[b] *College of Chemistry and Pharmacy Engineering, Nanyang Normal University, Nanyang, Henan, 473061, P. R. China*

*Corresponding authors: Guang-Zhen Liu, E-mail:gzliuly@126.com
Li-Ya Wang, E-mail: wlya@lynu.edu.cn

Physical measurements

Elemental analysis (C, H, N) was performed on a Flash EA 2000 elemental analyzer. Infrared spectrum (IR) was performed on a Nicolet 6700 FT-IR spectrophotometer over a range 4000-600 cm^{-1}. The thermo-gravimetric analyses (TGA) were performed on a SII EXStar6000 TG/DTA6300 analyzer under a dry nitrogen atmosphere with a heating rate of 10 °C min^{-1}. The powder X-ray diffraction patterns (PXRD) were recorded with a Bruker AXS D8 Advance diffractometer using monochromated $Cu_{K\alpha}$ radiation (λ = 1.5418 Å). All UV/vis spectra were recorded on a TU-1901 UV/vis spectrophotometer within the wavelength range 190–600 nm using the same solvent in the examined solution as a blank. Solid-state photodimerizations were carried out by performing UV-irradiation on the crystals using a 70 W UVA lamp and wavelength 365 nm as light source. The ^{1}H NMR measurements of the samples in d_6-DMSO solvent were carried out with an AVANCE AV 400MHz spectrometer.

Experimental Section

Synthesis of $1\cdot H_2O\cdot C_2H_5OH$

$Zn(OAc)_2\cdot 2H_2O$ (0.021 g, 0.10 mmol), 4-NO_2-bdc (0.021 g, 0.10 mmol), and bpe (0.036 g, 0.20 mmol) were dispersed in mixed solvent H_2O/EtOH (1:1; 7 mL), followed by the addition of KOH (0.006g, 0.10 mmol). The mixture was transferred to in a 23 mL Teflon liner stainless steel reactor and heated at 120°C for 4 days under static conditions, and then cooled to room temperature. Colourless block crystals were separated and washed with deionized water and allowed to dry in air (0.036 g, yield 85%). Elemental analysis calcd (%) for $C_{42}H_{36}N_6O_{16}Zn_3$: C 46.84, H 3.37, N 7.80; found: C 46.65, H 3.42, N 7.83. Selected IR (KBr, cm^{-1}): 3498(m), 3072(w), 1594(s), 1518(m), 1397(m), 1372(m), 1344(s), 1249(w), 1068(m), 1028(m), 1018(m), 922(w), 865(m), 838(m), 825(s), 787(m), 755(w), 732(w), 710(m), 666(m).

The single-crystal X-ray diffractions

The crystallographic data collections were carried out a Bruker SMART APEX II CCD diffractometer equipped with graphite-monochromated Mo_{Ka} radiation (λ = 0.71073 Å) at room temperature. CCDC 972455, 972456, 972457, 972458, 972459 contain the supplementary crystallographic data for this paper. These data can be obtained free of charge from The Cambridge Crystallographic Data Centre via www.ccdc.cam.ac.uk/data_request/cif.

Crystal data $\mathbf{1}\cdot H_2O\cdot C_2H_5OH$: Monoclinic, $C2/c$, a = 16.205(6) Å, b = 24.834(8) Å, c = 13.514(5) Å, β = 124.244(3)°, V = 4495.83 $Å^3$, Z = 4, ρ_{calcd} = 1.591 gcm^{-3}, μ(MoKα) = 1.666 mm^{-1}, GOF = 1.029, T = 296(2) K, Reflections collected data = 12933, Unique data = 4138, R_{int} = 0.0205, Observed data [$I > 2\sigma(I)$] = 3619, $R1$ = 0.0256, $wR2$ = 0.0701. Residual electron density: 0.480/-0.350 $eÅ^{-3}$.

Crystal data $\mathbf{1}\cdot H_2O\cdot 2.5H_2O$: Monoclinic, $C2/c$, a = 15.7066(13) Å, b = 25.077(2) Å, c = 13.4867(11) Å, β = 124.6280(10)°, V = 4371.0(6) $Å^3$, Z = 4, ρ_{calcd} = 1.636 gcm^{-3}, μ(MoKα) = 1.716 mm^{-1}, GOF = 1.061, T = 296(2) K, Reflections collected data = 13832, Unique data = 4056,

R_{int} = 0.0948, Observed data [$I > 2\sigma(I)$] = 2295, $R1$ = 0.0513, $wR2$ = 0.1002. Residual electron density: 0.488/-0.963 eÅ^{-3}.

Crystal data **1**·H_2O: Monoclinic, $C2/c$, a = 15.307(3) Å, b = 25.365(4) Å, c = 13.442(2) Å, β = 124.029(2)°, V = 4325.2(13) Å^3, Z = 4, ρ_{calcd} = 1.583 gcm^{-3}, μ(MoKα) = 1.726 mm^{-1}, GOF = 1.040, T = 296(2) K, Reflections collected data = 11937, Unique data = 4003, R_{int} = 0.0225, Observed data [$I > 2\sigma(I)$] = 3467, $R1$ = 0.0261, $wR2$ = 0.0622. Residual electron density: 0.304/-0.308 eÅ^{-3}.

Crystal data **1**·H_2O·I_2: Monoclinic, $C2/c$, a = 16.291(7) Å, b = 24.684(11) Å, c = 13.435(6) Å, β = 124.098(5)°, V = 4474(3) Å^3, Z = 4, ρ_{calcd} = 1.907 gcm^{-3}, μ(MoKα) = 3.051 mm^{-1}, GOF = 1.072, T = 296(2) K, Reflections collected data = 16323, Unique data = 4156, R_{int} = 0.0541, Observed data [$I > 2\sigma(I)$] = 2971, $R1$ = 0.0607, $wR2$ = 0.1581. Residual electron density: 0.903/-1.928 eÅ^{-3}.

Crystal data $[Zn_3(nbdc)_2(rctt\text{-tpcb})_{0.5}(bpe)_{0.5}(OH)_2]\cdot H_2O\cdot 0.5H_2O$ (**2**): Triclinic, P-1, a = 13.838(19) Å, b = 13.844(19) Å, c = 14.42(3) Å, α = 108.31(2)°, β = 110.43(2)°, γ = 107.046(16)° , V = 2191(7) Å^3, Z = 2, ρ_{calcd} = 1.574 gcm^{-3}, μ(MoKα) = 1.705 mm^{-1}, GOF = 0.911, T = 296(2) K, Reflections collected data = 16335, Unique data = 8063, R_{int} = 0.3079, Observed data [$I > 2\sigma(I)$] = 1790, $R1$ = 0.1092, $wR2$ = 0.2503. Residual electron density: 0.799/-0.809 eÅ^{-3}.

Table S1 Crystal data and refinement parameters for **1**·H_2O·C_2H_5OH, **1**·H_2O·2.5H_2O, **1**·H_2O, **1**·H_2O·I_2, and **2**

	1·H_2O·C_2H_5OH	**1**·H_2O·2.5H_2O	**1**·H_2O	**1**·H_2O·I_2	**2**
Empirical formula	$C_{42}H_{36}N_6O_{16}Zn_3$	$C_{40}H_{35}N_6O_{17.5}Zn_3$	$C_{40}H_{30}N_6O_{15}Zn_3$	$C_{40}H_{30}I_2N_6O_{15}Zn_3$	$C_{40}H_{31}N_6O_{15.50}Zn_3$
Formula weight	1076.88	1075.86	1030.82	1284.62	1039.81
Crystal system	Monoclinic	Monoclinic	Monoclinic	Monoclinic	Triclinic
Space group	*C2/c*	*C2/c*	*C2/c*	*C2/c*	*P*-1
a (Å)	16.205(6)	15.7066(13)	15.307(3)	16.291(7)	13.838(19)
b (Å)	24.834(8)	25.077(2)	25.365(4)	24.684(11)	13.844(19)
c (Å)	13.514(5)	13.4867(11)	13.442(2)	13.435(6)	14.42(3)
a (°)	90.00	90.00	90.00	90	108.31(2)
β (°)	124.244(3)	124.6280(10)	124.029(2)	124.098(5)	110.43(2)
γ (°)	90.00	90.00	90.00	90	107.046(16)
Volume (Å^3)	4495.83	4371.0(6)	4325.2(13)	4474(3)	2191(7)
Z	4	4	4	4	2
D_{calc} (g cm^{-3})	1.591	1.636	1.583	1.907	1.574
μ (mm^{-1})	1.666	1.716	1.726	3.051	1.705
F(000)	2192	2192	2088	2512	1052
θ range (°)	2.45 - 25.50	2.45 - 25.50	2.43 - 25.50	2.46 - 25.50	2.47 - 25.50
Reflections collected	12933	13832	11937	16323	16335
Independent reflections	4138	4056	4003	4156	8063
R(*int*)	0.0205	0.0948	0.0225	0.0541	0.3079
Data/restraints/parameters	4138 / 0 / 321	4056 / 0 / 308	4003 / 0 / 293	4156 / 0 / 312	8063 / 0 / 589
Goodness-of-fit	1.029	1.061	1.040	1.072	0.911
R_1	0.0256	0.0513	0.0261	0.0607	0.1092
wR_2 [$I>2\sigma(I)$]	0.0701	0.1002	0.0622	0.1581	0.2503
R_1 (all data)	0.0318	0.1249	0.0342	0.0908	0.3720
wR_2 (all data)	0.0740	0.1245	0.0648	0.1752	0.3804
$\Delta\rho_{max}$ and $\Delta\rho_{min}$(e.Å^{-3})	0.480 / -0.350	0.488 / -0.963	0.3042 / -0.308	0.903 / -1.928	0.799 / -0.809

Table S2 The selected bond lengths (Å) and bond angles (º) for **1**·H_2O·C_2H_5OH, **1**·H_2O·2.5H_2O, and **1**·H_2O[a]

1·H_2O·C_2H_5OH		**1**·H_2O·2.5H_2O		**1**·H_2O	
Zn(1)-O(7)	2.0429(15)	Zn(1)-O(7)	2.047(4)	Zn(1)-O(7)	2.0386(14)
Zn(1)-N(2)	2.1717(18)	Zn(1)-N(2)	2.173(4)	Zn(1)-N(2)	2.1671(17)
Zn(1)-O(3)	2.1763(17)	Zn(1)-O(3)	2.186(4)	Zn(1)-O(3)	2.1745(15)
Zn(2)-O(7)	1.8881(16)	Zn(2)-O(7)	1.881(4)	Zn(2)-O(7)	1.8871(15)
Zn(2)-O(4)#1	1.9877(17)	Zn(2)-O(4)#1	1.981(4)	Zn(2)-O(4)#1	1.9786(16)
Zn(2)-O(1)#2	1.9805(17)	Zn(2)-O(1)#2	1.983(4)	Zn(2)-O(1)#2	1.9804(15)
Zn(2)-N(3)#3	2.0652(19)	Zn(2)-N(3)#3	2.055(4)	Zn(2)-N(3)#3	2.0613(18)
O(7)#1-Zn(1)-O(7)	180.00(12)	O(7)-Zn(1)-O(7)#1	180.0(2)	O(7)-Zn(1)-O(7)#1	180.00(11)
O(7)#1-Zn(1)-N(2)#1	90.40(7)	O(7)-Zn(1)-N(2)#1	89.68(15)	O(7)-Zn(1)-N(2)	90.38(6)
O(7)-Zn(1)-N(2)#1	89.60(7)	O(7)#1-Zn(1)-N(2)#1	90.32(15)	O(7)#1-Zn(1)-N(2)	89.62(6)
O(7)#1-Zn(1)-N(2)	89.60(7)	O(7)-Zn(1)-N(2)	90.32(15)	O(7)-Zn(1)-N(2)#1	89.62(6)
O(7)-Zn(1)-N(2)	90.40(7)	O(7)#1-Zn(1)-N(2)	89.68(15)	O(7)#1-Zn(1)-N(2)#1	90.38(6)
N(2)#1-Zn(1)-N(2)	180.00(11)	N(2)#1-Zn(1)-N(2)	180.0(3)	N(2)-Zn(1)-N(2)#1	180.00(10)
O(7)#1-Zn(1)-O(3)#1	88.92(6)	O(7)-Zn(1)-O(3)	89.91(15)	O(7)-Zn(1)-O(3)	90.27(6)
O(7)-Zn(1)-O(3)#1	91.08(6)	O(7)#1-Zn(1)-O(3)	90.09(15)	O(7)#1-Zn(1)-O(3)	89.73(6)
N(2)#1-Zn(1)-O(3)#1	91.52(7)	N(2)#1-Zn(1)-O(3)	88.24(16)	N(2)-Zn(1)-O(3)	91.82(6)
N(2)-Zn(1)-O(3)#1	88.48(7)	N(2)-Zn(1)-O(3)	91.76(16)	N(2)#1-Zn(1)-O(3)	88.18(6)
O(7)#1-Zn(1)-O(3)	91.08(6)	O(7)-Zn(1)-O(3)#1	90.09(15)	O(7)-Zn(1)-O(3)#1	89.73(6)
O(7)-Zn(1)-O(3)	88.92(6)	O(7)#1-Zn(1)-O(3)#1	89.91(15)	O(7)#1-Zn(1)-O(3)#1	90.27(6)
N(2)-Zn(1)-O(3)	91.52(7)	N(2)#1-Zn(1)-O(3)#1	91.76(16)	N(2)#1-Zn(1)-O(3)#1	91.82(6)
N(2)#1-Zn(1)-O(3)	88.48(7)	N(2)-Zn(1)-O(3)#1	88.24(16)	N(2)-Zn(1)-O(3)#1	88.18(6)
O(3)#1-Zn(1)-O(3)	180.00(11)	O(3)#1-Zn(1)-O(3)	180.0(2)	O(3)-Zn(1)-O(3)#1	180.00(9)
O(7)-Zn(2)-O(1)#2	106.45(7)	O(7)-Zn(2)-O(4)#1	106.94(16)	O(7)-Zn(2)-O(4)#1	106.66(7)
O(7)-Zn(2)-O(4)#1	127.05(7)	O(7)-Zn(2)-O(1)#2	126.39(16)	O(7)-Zn(2)-O(1)#2	126.45(7)
O(1)#2-Zn(2)-O(4)#1	98.79(7)	O(4)#1-Zn(2)-O(1)#2	98.83(16)	O(4)#1-Zn(2)-O(1)#2	100.67(6)
O(7)-Zn(2)-N(3)#3	115.73(7)	O(7)-Zn(2)-N(3)#3	115.49(17)	O(7)-Zn(2)-N(3)#3	115.01(7)
O(4)#1-Zn(2)-N(3)#3	105.02(8)	O(4)#1-Zn(2)-N(3)#3	105.03(18)	O(4)#1-Zn(2)-N(3)#3	104.98(8)
O(1)#2-Zn(2)-N(3)#3	100.86(7)	O(1)#2-Zn(2)-N(3)#3	101.34(17)	O(1)#2-Zn(2)-N(3)#3	100.57(7)

[a] Symmetry transformations used to generate equivalent atoms: #1 –x + 1, -y, -z; #2 –x + 1, y, -z - 1/2; #3 –x + 1/2, -y + 1/2, -z.

Table S3 The selected bond lengths (Å) and bond angles (º) for **1**·H_2O·I_2[a] and **2**[b]

1·H_2O·I_2		**2**			
Zn(1)-O(7)	2.033(4)	Zn(1)-O(14)	1.873(15)	Zn(3)-O(7)#2	2.007(13)
Zn(1)-N(2)	2.172(5)	Zn(1)-O(1)	1.934(15)	Zn(3)-O(7)	2.007(13)
Zn(1)-O(3)	2.180(5)	Zn(1)-O(9)#1	1.965(16)	Zn(3)-O(3)	2.094(17)
Zn(2)-O(7)	1.878(5)	Zn(1)-N(1)	2.090(19)	Zn(3)-O(3)#2	2.094(17)
Zn(2)-O(4)#2	1.992(5)	Zn(2)-O(14)	2.026(12)	Zn(3)-N(4)	2.21(2)
Zn(2)-O(1)#3	1.964(5)	Zn(2)-O(14)#1	2.026(12)	Zn(3)-N(4)#2	2.21(2)
Zn(2)-N(3)#4	2.058(6)	Zn(2)-O(8)	2.101(17)	Zn(4)-O(7)	1.885(16)
I(1)-I(1)#1	2.56(2)	Zn(2)-O(8)#1	2.101(17)	Zn(4)-O(11)	1.962(16)
I(2)-I(2)#1	2.625(5)	Zn(2)-N(2)#1	2.223(19)	Zn(4)-O(4)#2	1.977(17)
		Zn(2)-N(2)	2.223(19)	Zn(4)-N(3)	2.04(2)
O(7)#2-Zn(1)-O(7)	180.0(2)	O(14)-Zn(1)-O(1)	130.7(7)	O(7)#2-Zn(3)-O(7)	180.000(4)
O(7)#2-Zn(1)-N(2)	89.91(19)	O(14)-Zn(1)-O(9)#1	104.3(6)	O(7)#2-Zn(3)-O(3)	91.3(6)
O(7)-Zn(1)-N(2)	90.09(19)	O(1)-Zn(1)-O(9)#1	100.0(7)	O(7)-Zn(3)-O(3)	88.7(6)
O(7)#2-Zn(1)-N(2)#2	90.09(19)	O(14)-Zn(1)-N(1)	113.6(7)	O(7)#2-Zn(3)-O(3)#2	88.7(6)
O(7)-Zn(1)-N(2)#2	89.91(19)	O(1)-Zn(1)-N(1)	100.4(7)	O(7)-Zn(3)-O(3)#2	91.3(6)
N(2)-Zn(1)-N(2)#2	180.000(1)	O(9)#1-Zn(1)-N(1)	104.5(8)	O(3)-Zn(3)-O(3)#2	180.0(6)
O(7)#2-Zn(1)-O(3)	90.55(18)	O(14)-Zn(2)-O(14)#1	180.000(4)	O(7)#2-Zn(3)-N(4)	88.4(7)
O(7)-Zn(1)-O(3)	89.45(18)	O(14)-Zn(2)-O(8)	89.2(6)	O(7)-Zn(3)-N(4)	91.6(6)
N(2)-Zn(1)-O(3)	91.4(2)	O(14)#1-Zn(2)-O(8)	90.8(6)	O(3)-Zn(3)-N(4)	87.6(8)
N(2)#2-Zn(1)-O(3)	88.6(2)	O(14)-Zn(2)-O(8)#1	90.8(6)	O(3)#2-Zn(3)-N(4)	92.4(8)
O(7)#2-Zn(1)-O(3)#2	89.45(18)	O(14)#1-Zn(2)-O(8)#1	89.2(6)	O(7)#2-Zn(3)-N(4)#2	91.6(6)
O(7)-Zn(1)-O(3)#2	90.55(18)	O(8)-Zn(2)-O(8)#1	180.0(8)	O(7)-Zn(3)-N(4)#2	88.4(6)
N(2)-Zn(1)-O(3)#2	88.6(2)	O(14)-Zn(2)-N(2)#1	88.8(6)	O(3)-Zn(3)-N(4)#2	92.4(8)
N(2)#2-Zn(1)-O(3)#2	91.4(2)	O(14)#1-Zn(2)-N(2)#1	91.2(6)	O(3)#2-Zn(3)-N(4)#2	87.6(8)
O(3)-Zn(1)-O(3)#2	180.0	O(8)-Zn(2)-N(2)#1	89.6(6)	N(4)-Zn(3)-N(4)#2	180.000(4)
O(7)-Zn(2)-O(4)#2	107.7(2)	O(8)#1-Zn(2)-N(2)#1	90.4(6)	O(7)-Zn(4)-O(11)	131.2(8)
O(7)-Zn(2)-O(1)#3	126.3(2)	O(14)-Zn(2)-N(2)	91.2(6)	O(7)-Zn(4)-O(4)#2	103.9(6)
O(1)#3-Zn(2)-O(4)#2	98.7(2)	O(14)#1-Zn(2)-N(2)	88.8(6)	O(11)-Zn(4)-O(4)#2	99.4(8)
O(7)-Zn(2)-N(3)#4	116.0(2)	O(8)-Zn(2)-N(2)	90.4(6)	O(7)-Zn(4)-N(3)	115.2(9)
O(4)#2-Zn(2)-N(3)#4	105.0(2)	O(8)#1-Zn(2)-N(2)	89.6(6)	O(11)-Zn(4)-N(3)	99.9(9)
O(1)#3-Zn(2)-N(3)#4	100.3(2)	N(2)#1-Zn(2)-N(2)	180.000(3)	O(4)#2-Zn(4)-N(3)	103.3(9)

[a] Symmetry transformations used to generate equivalent atoms: #1 –x + 1, -y, -z; #2 –x + 1, y, -z - 1/2; #3 –x + 1/2, -y + 1/2, -z; #4 –x - 1/2, -y + 3/2, -z.

[b] Symmetry transformations used to generate equivalent atoms: #1 –x + 2, -y + 1, -z + 1; #2 –x + 1, -y + 1, -z + 1; #3 –x + 2, -y + 1, -z; #4 -x, -y, -z.

Various SC-SC desolvated-resolvated structural transformations

When heating sample at 120°C, all solvent H_2O and EtOH molecules in both cages can be completely evacuated along the Route **a** (Fig. 1), however, the solvent-free phase **1** is hard to be captured because a rapid rehydration process is completed within several minutes in air along the Route **b**. The dynamic H_2O uptake of **1** in air was examined by well-designed cyclic TGA (Fig. S9, ESI†) and IR spectra (Fig. S10, ESI†). Firstly, bring the crystal **1**·H_2O·C_2H_5OH to 140°C operated on the TGA apparatus in high purity N_2 stream, and then slowly reduce the heat to the room temperature. After that, the sample chamber of the TGA apparatus is opened with the crystals exposed to air for a period of time, followed by next cyclic TGA experiment to measure its water content, the time-dependent hydration of **1** is recorded as H_2O content plotted against exposed time. It is noted that the crystals can reserve the crystallinity after eight TGA run. The time-dependent hydration of **1** showed that a fast H_2O adsorption occurred before ~1 min (1.83 wt%, corresponding to 1.03H_2O for three Zn atoms), followed by a relatively slow H_2O uptake, finally reaching the saturation within 10 min (5.8 wt%, corresponding to 3.46H_2O for three Zn atoms) to give a hydrated phase **1**·H_2O·2.5H_2O (Table S1, ESI†) with one H_2O molecule located in cage A and 2.5H_2O molecules accommodated in cage B.

Fortunately, we succeeded in capturing an intermediate during the hydration of **1** in first ~1min giving a partly hydrated phase $[Zn_3(nbdc)_2(bpe)_2(OH)_2]\cdot H_2O$ (**1**·H_2O) (Table S1, ESI†). The intermediate of the hydration evolution of **1** is obtained in a more tricky way that a single crystal of **1**·H_2O·2.5H_2O is fixed in a glass capillary and heated at 120°C for 0.5h, followed by exposure to air humidity for ~1 min then continuous aeration of high purity N_2 stream, finally sealed at both ends promptly. The SCXRD analysis shows that one H_2O molecule occupies cage A leaving cage B still empty in **1**·H_2O. It clearly shows that the water molecules firstly fill the smaller cage A, then occupy the larger cage B during the hydration along the Route **c** and **d**, that is, **1**·H_2O is the intermediate from **1** to **1**·H_2O·2.5H_2O. It is reasonable to propose that water molecule can diffuse into the cage A from the cage B through the side window between them, considering that the cage A has no pore opening in the crystal surface to allow for the direct access

of guest molecule. The filling of the smaller then the larger adsorption sites is consistent with the theory of micropore filling, indicating a two-step pore-filling sequence. Alternatively, the intermediate **1**·H_2O could not be arrested by performing usual heating on **1**·H_2O·2.5H_2O along the supposed the Route **e** because all water guests accommodated in both cages nearly lose instantly along the Route **f**, though it is realistic that **1**·H_2O can convert to **1** by performing heating along the Route **g**. Such fast water adsorption behavior in air in a SC-SC manner is a rarely observed phenomenon in coordination polymers.

Furthermore, the exposure of crystal **1** to mixed EtOH/H_2O vapours makes it restore to **1**·H_2O·C_2H_5OH in a SC-SC manner along the Route **h**. This process is realized by bringing the crystal **1**·H_2O·C_2H_5OH to 140^{o}C in high purity N_2 stream, and then slowly reduce the heat to the room temperature. After that, the crystals are exposed to the mixed EtOH/H_2O vapors for 30min.

Thiosulfate determination of the iodine content

The iodine-loaded crystals (50 mg) were soaked in a 5 ml of iodine cyclohexane solution (0.1 M/L). After the uptake of iodine, the resulting violet crystals were separated from the iodine solution and thoroughly washed with cyclohexane, and then dried in air. Then these crystals were soaked in ethanol solution (50 mL), and thiosulfate determination of iodine content in the solution.

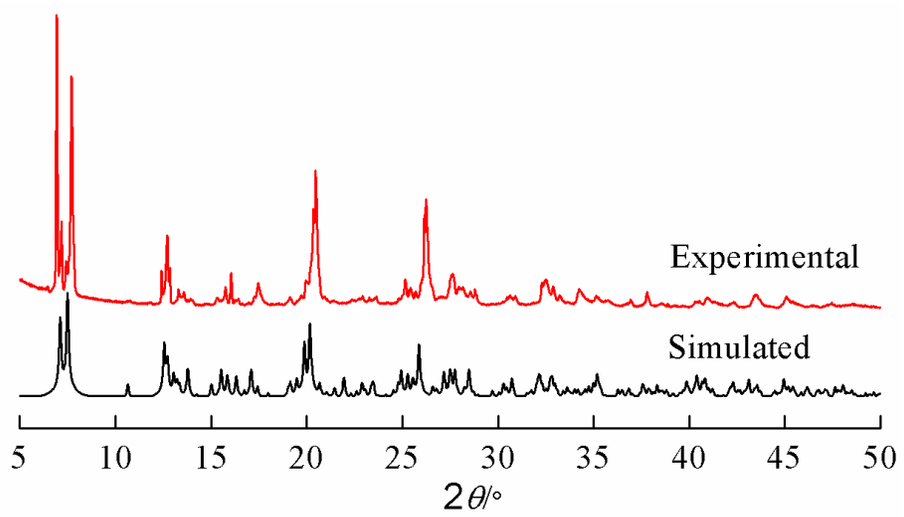

Fig. S1. The experimental and simulated PXRD patterns for **1**·H_2O·C_2H_5OH.

Crystal structure of $1\cdot H_2O\cdot C_2H_5OH$

The SCXRD revealed that $1\cdot H_2O\cdot C_2H_5OH$ consists of a linear trinuclear $[Zn_3N_4(\mu_2\text{-}OH)_2(COO)_4]$ cluster that dictates the overall framework topology of $(6^5.8)$ *cds*. Each linear trimeric unit $[Zn_3N_4(\mu_2\text{-}OH)_2(COO)_4]$ (Fig. S2) consists of two crystallographically unique Zn(II) atoms with octahedral Zn(1) atom locating in the inversed centre symmetrically double-bridged to two terminal tetrahedral Zn(2) atoms through the combination of one μ_2-OH bridge and one μ_2-η^1:η^1-COO bridge, respectively. The adjacent trimeric units are further double-bridged by two μ_2-nbdc ligands propagating along the *c* direction to form 1D Zn-carboxylate ribbons (Fig. S3), which are finally cross-linked by parallel positioned bpe pairs with four peripheral ribbons to afford its 3D framework containing 1D open channel with "Chinese-Spindle-like" pore opening (Fig. S4). Noticeably, the $-NO_2$ groups of nbdc anions are penetrated into the inner of the channel making its appearing in three parts. Actually, there exist two types of cage-like structures, identified as A and B, respectively, of which two smaller cages A at the channel corners possess a triangular prism-like shape enclosed mainly by four bpe and two nbdc linkers, and the larger cage B at the channel centre possesses a sphere-like shape surrounded primarily by four nbdc linkers (Fig. S5). The cages B stack along the *c* direction forming 1D open channel with circular aperture, but the cage A has no visible pore opening in the crystal surface except for communicating with the adjacent cage B through the side window between them along the *b* direction. Each unit cell contains four cages (2A and 2B) with each cage A occupied by one H_2O molecule and each cage B filled with one EtOH molecule disordered over two positions (Fig. S6).

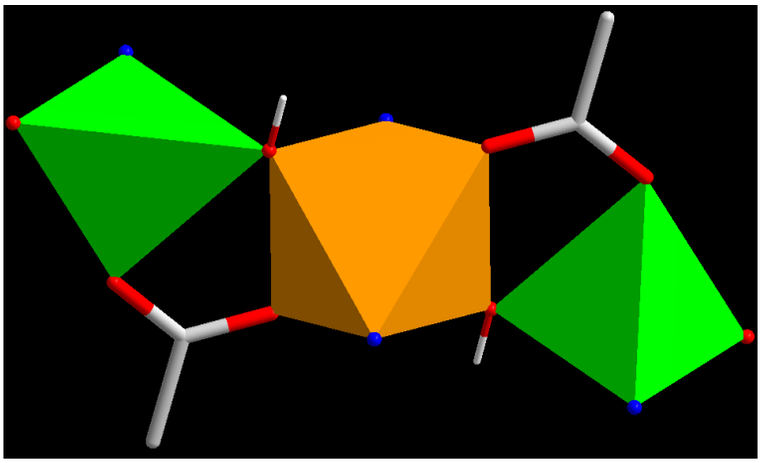

Fig. S2. The linear trinuclear $[Zn_3N_4(\mu_2\text{-}OH)_2(COO)_4]$ unit in **1**·H_2O·C_2H_5OH.

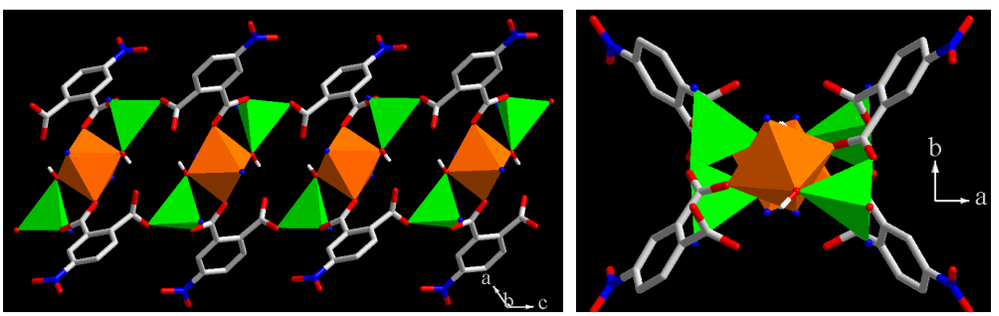

(a) (b)

Fig. S3. 1D Zn-carboxylate ribbons propagating along the *c* direction: (a) Side view; (b) Top view.

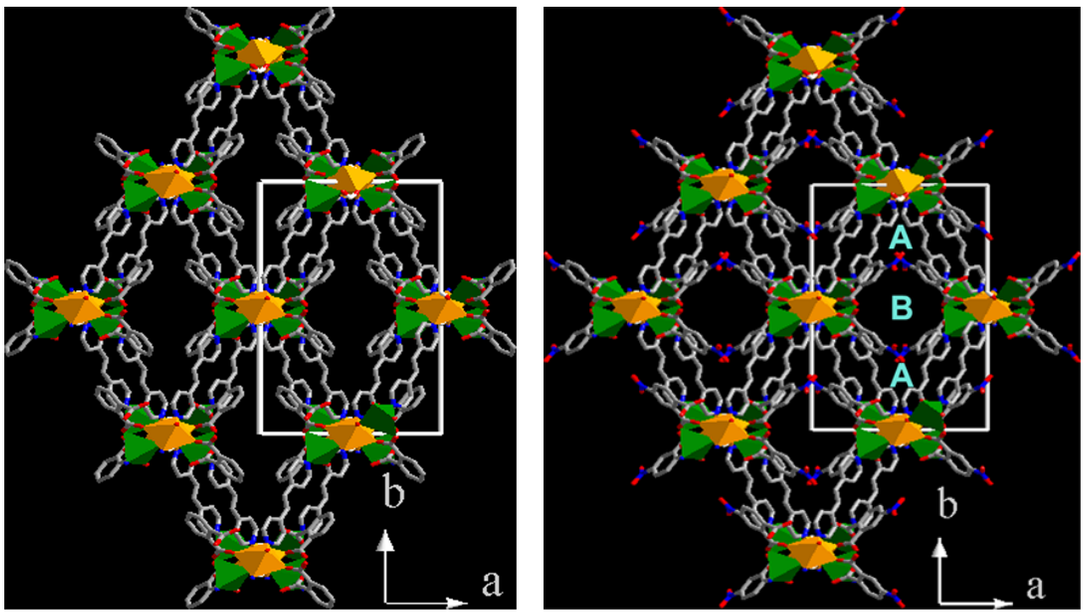

Fig. S4. (a) A portion of the 3D framework of **1**·H_2O·C_2H_5OH with "Chinese-Spindle-like" aperture viewed along *c*-axis. Hydrogen atoms and –NO_2 groups are omitted for clarity. (b) Crystal structure of **1**·H_2O·C_2H_5OH viewed along *c* axis indicating –NO_2 groups oriented towards pore to form two types of cage-like structures marked as A at the channel corner and B at the channel centre. C gray, N blue, O red, tetrahedral Zn green and octahedral Zn orange. Solvent H_2O at cage A, solvent EtOH at cage B, and hydrogen atoms are omitted for clarity.

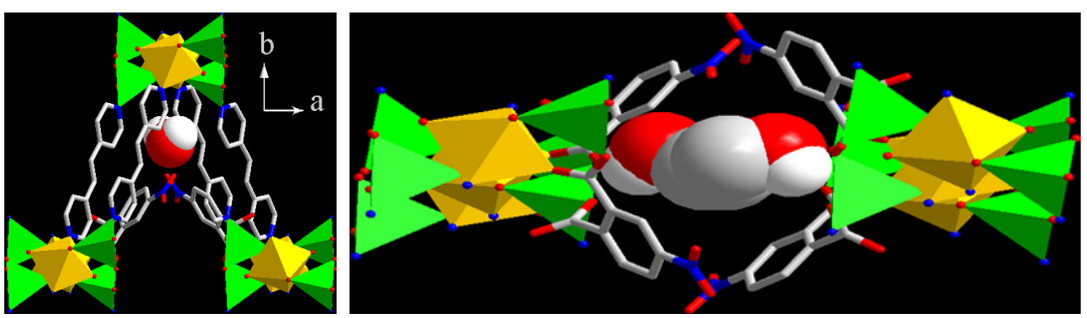

Cage A Cage B

Fig. S5. Two types of cage-like structures identified as cage A occupied by one H_2O molecule and cage B occupied by one EtOH molecule disordered over two positions.

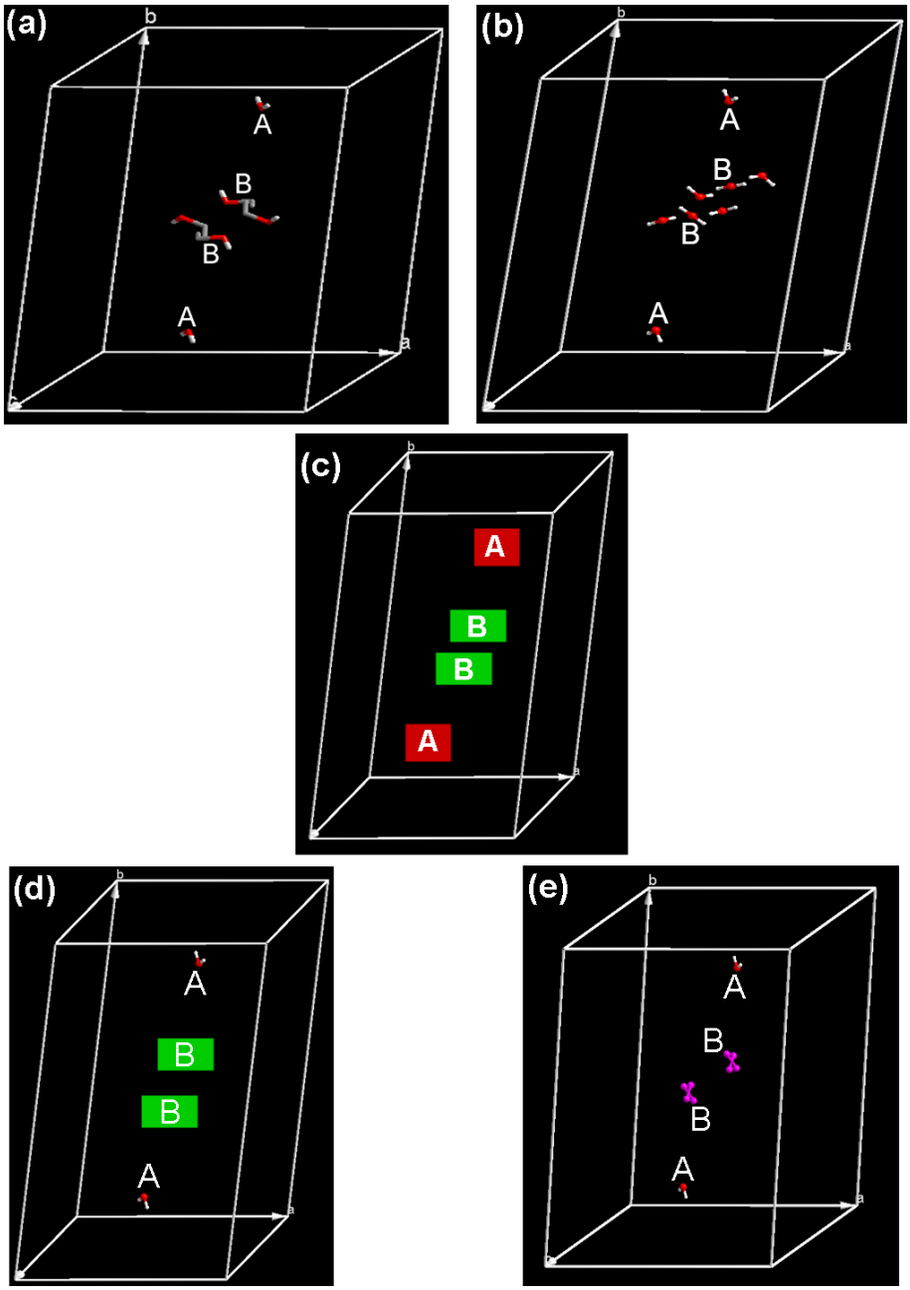

Fig. S6. Simplified representation of a unit cell with two cage A and two cage B labeled: (a) **1**·H_2O·C_2H_5OH with two A sites occupied by H_2O molecule and two B sites accommodated by disordered EtOH molecule; (b) **1**·H_2O·2.5H_2O with two A sites occupied by H_2O molecule and two B sites accommodated by disordered 2.5H_2O molecules; (c) **1** with both two A sites and two B sites empty; (d) **1**·H_2O with two A sites occupied by H_2O molecule and two empty B sites; (e) **1**·H_2O·I_2 with two A sites occupied by H_2O molecule and two B sites accommodated by disordered I_2 molecule.

TGA of 1·H_2O·C_2H_5OH

TGA (Fig. S7) of **1**·H_2O·C_2H_5OH showed that an initial mass loss of 5.9% from solvent water and ethanol incorporated in both cages is evident from the room temperature to 120°C (calcd. 6.0%), followed by a stable plateau after which the decomposition of the organic ligands occurs between 245 and 620°C with a series of thermal events. The observed mass remnant of 22.9% at 900°C represents the deposition of ZnO component, which is well agreement with the calculated value of 22.7%. The air-stable crystals of **1**·H_2O·C_2H_5OH can maintain good crystallinity and framework integrity at least before 240°C, which was verified by variable-temperature powder X-ray diffractions (VT-PXRD).

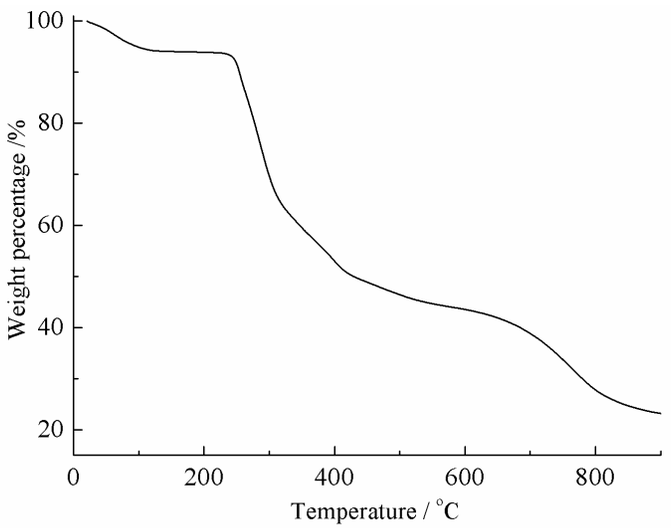

Fig. S7. The TGA curve for **1**·H_2O·C_2H_5OH.

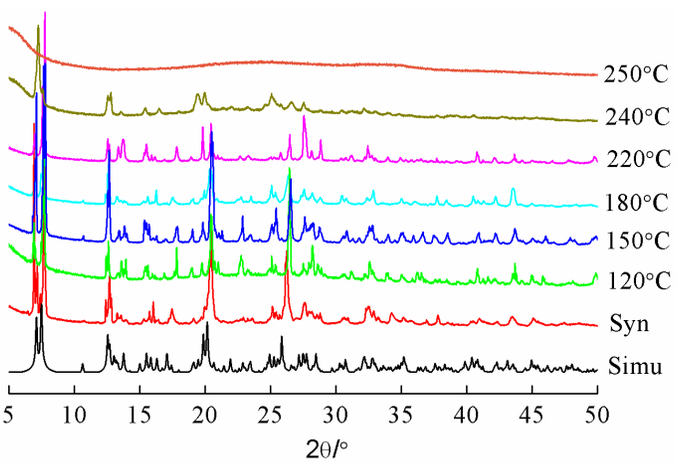

Fig. S8. Variable-temperature powder X-ray diffractions (VT-PXRD) for **1**·H_2O·C_2H_5OH.

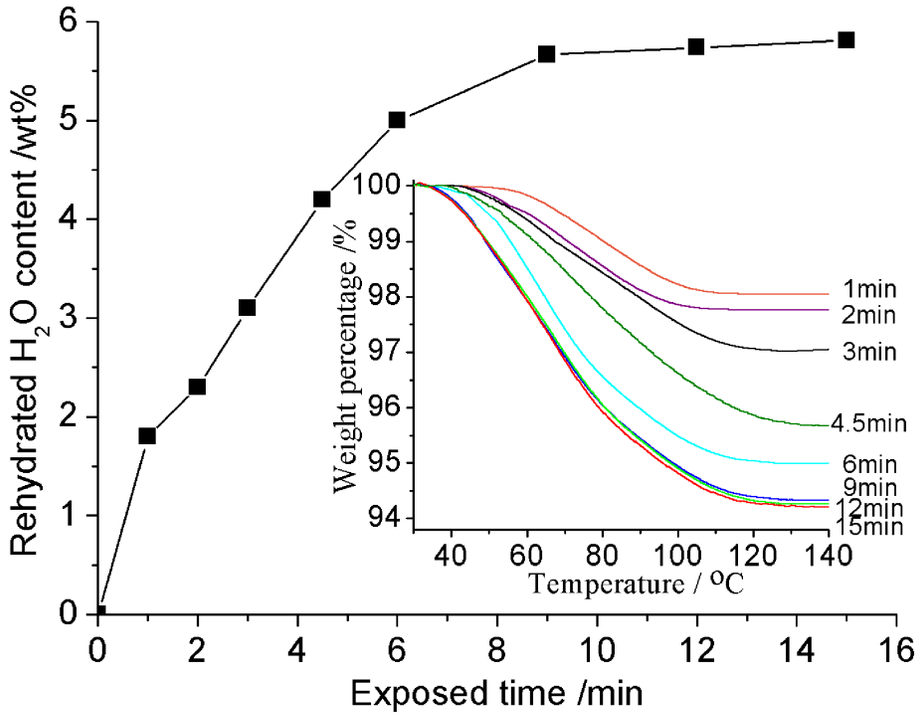

Fig. S9. The time-dependent H_2O uptake of **1** at ambient atmosphere reaching complete conversion to **1**·H_2O·2.5H_2O after saturation adsorption within 10 min. Insert: Time-resolved TGA curves of **1** exposed to air for different durations.

Time-dependent IR spectra

IR spectra for **1**·H_2O·2.5H_2O shows obvious adsorption bands of water in the region 3450−3650 cm^{-1}, but their strength extremely weaken upon dehydration and the existence of residual water IR adsorption is attributed to stretching vibration of hydroxyl groups of the framework. Time-dependent IR spectra of **1** upon exposure to air humidity for different durations (Fig. S10) shows that adsorption bands of water are gradually restored to the initial intensity of **1**·H_2O·2.5H_2O within several minutes. Other main adsorption bands remain unchanged, also demonstrating that the host backbone is preserved even if it undergone a guest evacuated-uploaded cycle.

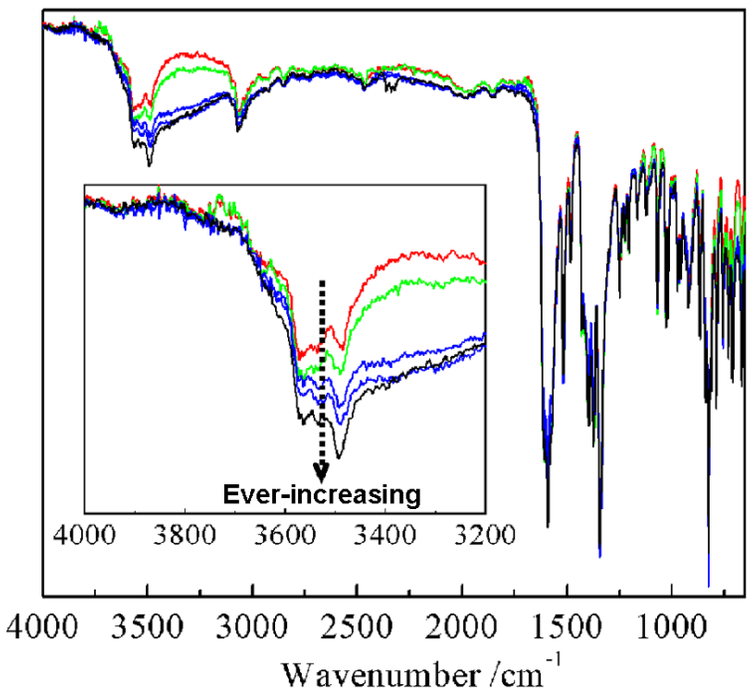

Fig. S10. Time-dependent IR spectra of **1** exposed in air for different durations. Color code: red line, 1min; green line, 3 min; blue, 6min; cyan line, 9min; black line, 12min. Insert: the amplified water adsorption.

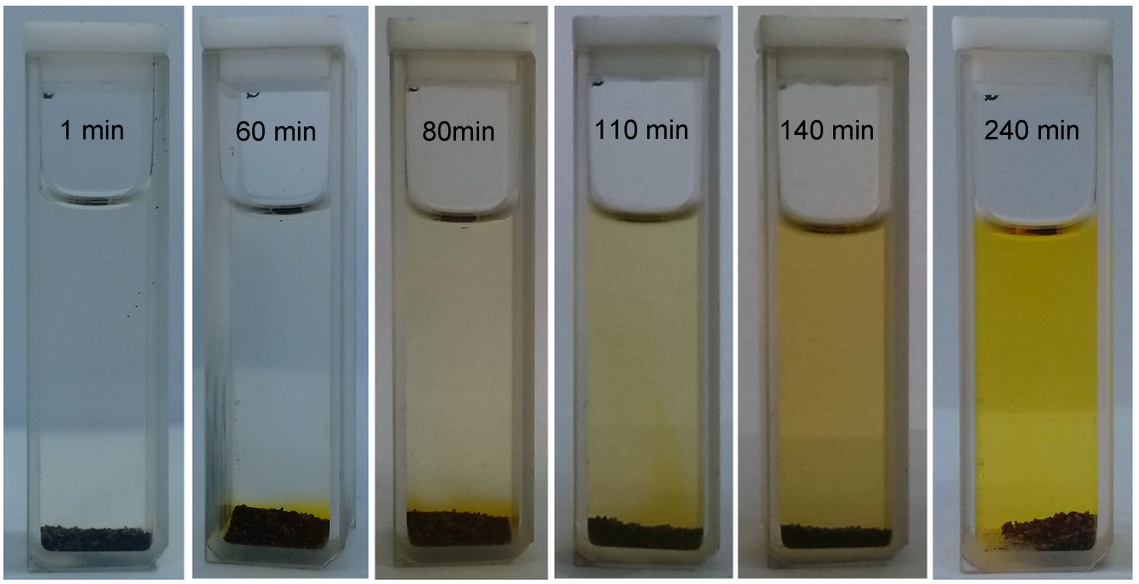

Fig. S11. Photographs showing progress of the iodine release from **1**·H_2O·I_2 when the I_2-loaded crystals were immersed in ethanol for different durations.

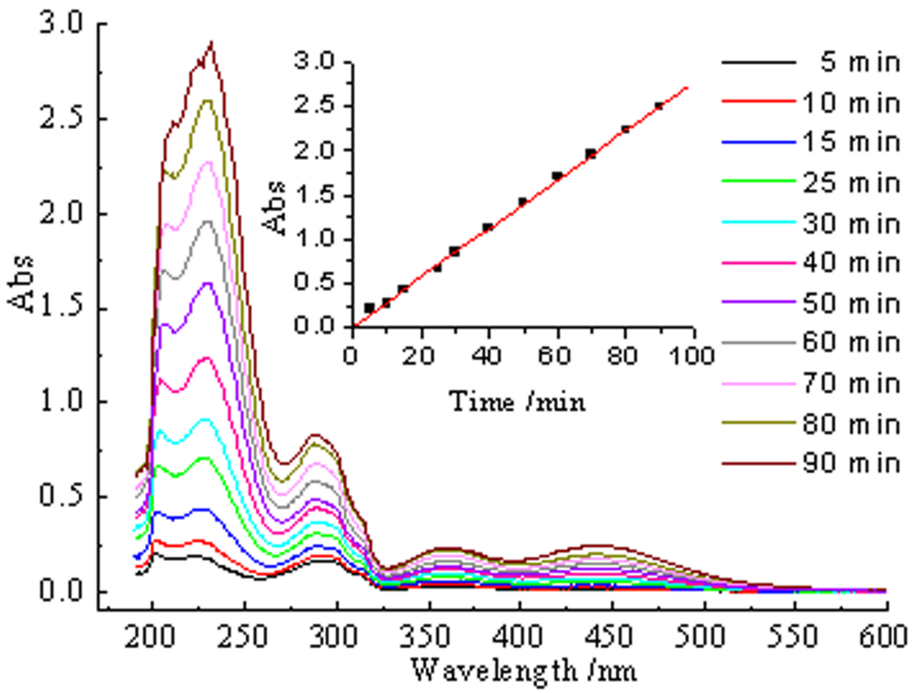

Fig. 12. Temporal evolution of UV/vis absorption spectra for the delivery of iodine from iodine-loaded sample in the first 90min. Insert: fit curve of the controlled delivery of iodine.

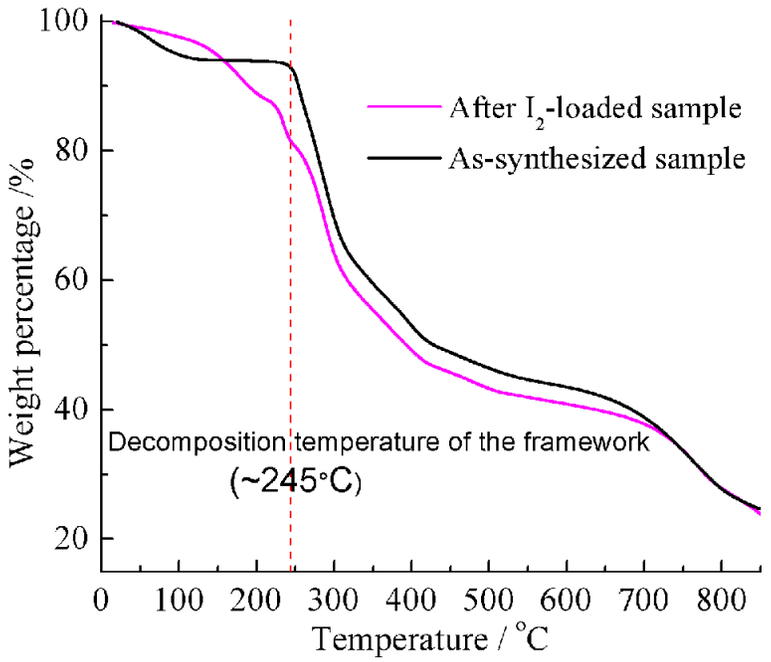

Figure S13. The TGA curves for **1**·H_2O·C_2H_5OH and **1**·H_2O·I_2.

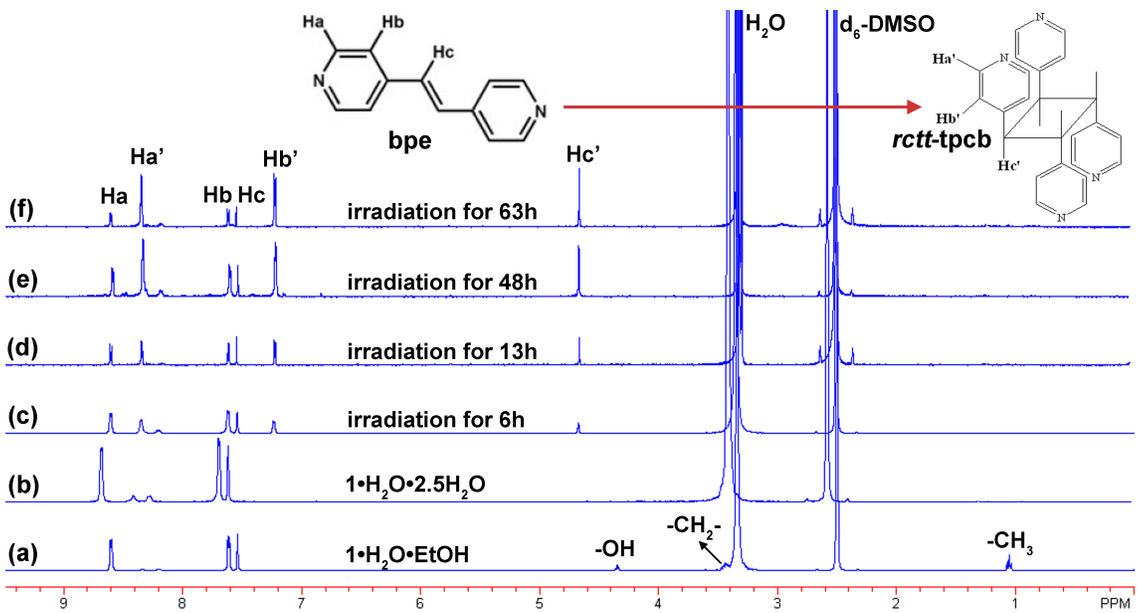

Fig. S14. The ^{1}H NMR spectra: (a) As-synthesized sample **1**·H_2O·C_2H_5OH; (b) The desolvated-rehydrated sample **1**·H_2O·$2.5H_2O$; (c)-(f) The photoreactive products for different irradiation time.

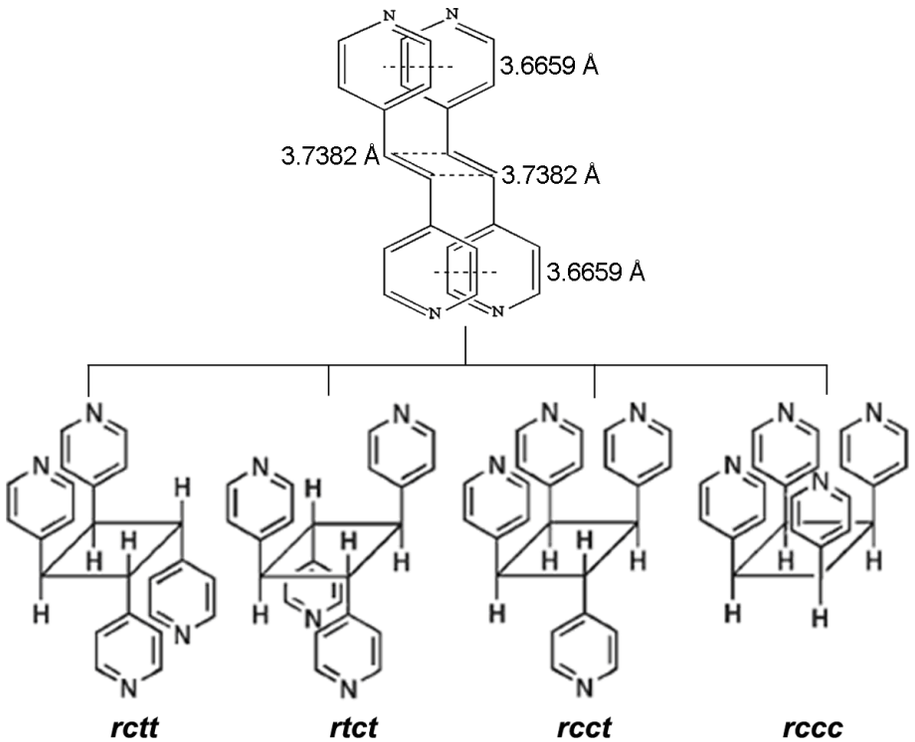

Fig. S15. Pictorial representations of four possible regioisomers of *tpcb* upon undergoing photochemical [2+2] cycloaddition reaction between two parallel positioned bpe molecules. Spatial relative positions of a pair of bpe ligands in **1**·H_2O·C_2H_5OH are labeled (dotted lines).

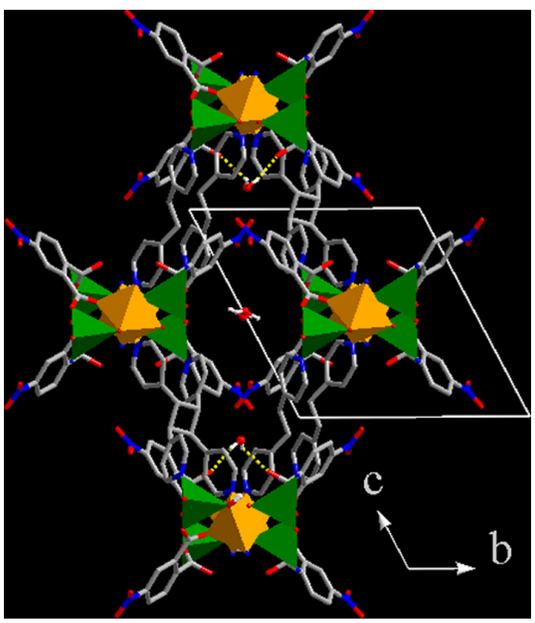

Fig. S16. The structure of the 50% photoreactive product **2** viewed along *a* direction.